Guidance and control of an overactuated autonomous surface platform for diver tracking

Nikola Mišković, Đula Nađ, Nikola Stilinović and Zoran Vukić

***Abstract*— The high-risk nature of SCUBA diving activities is usually dealt with by pairing up divers and adopting well defined rules for diving operations to reduce the chance of accidents. However, during more challenging dives (such as technical dives) these procedures may not be sufficient to ensure almost accident-free operations, for the divers must manoeuvre in complex 3D environments, carry cumbersome equipment, and focus attention on operational details. Technological advancement and research related to diver safety, navigation and monitoring has been identified as crucial for advancing diving activities. This paper reports current state of research performed at UNIZG–FER related to an autonomous overactuated surface platform used for following divers and transmitting GPS signal to the underwater. The implemented guidance and control algorithms are described and simulations obtained on realistic models developed in the ROS environment are provided. Special attention is given to algorithms for diver tracking by using measurements from a USBL. Diver motion estimators are used to improve the performance of the sparse and noisy USBL measurements. The results presented in this paper are a starting point for in-the-field experiments expected to take place in the real-world environment.**

I. Introduction

SCUBA diving activities, weather they are recreational, scientific or technical, are classified as high-risk due to i) unpredictable, dangerous and unfamiliar environment constantly under influence of external disturbances; ii) dependency on technical equipment that ensures life support; and iii) health consequences that diving can have on a diver. In strong collaboration with professional and recreational divers, three major issues that emerge during classical diver operations have been identified: diver safety, diver underwater navigation and diver monitoring from the surface. *Diver safety*, as the most important aspect, is seriously jeopardized during diving activity not only because of unpredictable underwater scenarios, but also because of diver invisibility to surface vessels. Currently, diving areas are marked by using passive buoys that serve as indicators for man operated surface vessels to avoid this area. Area of operation can be increased if the diving buoy is linked to the diver via a cable - this solution is unacceptable for deeper and long dives due to possible entanglement, drag and cumbersomeness. *Underwater navigation* poses a challenge even for experienced divers. Classical techniques of underwater navigation, such as referencing according to the sun, compass, underwater features, are imprecise and tedious, and require significant amount of concentration and experience. Current technological solutions enable determining position of the diver relative to the surface station by using acoustic based technology. These systems, that rely on static transmitters/receivers, exhibit serious performance deterioration when the diver is distanced from the ship. Another identified issue is related to diver *monitoring from the surface*. This issue is important to diving supervisors who monitor the progress of diving operations, as well as divers themselves who appreciate monitoring as a way of increasing their safety during the dives. Current systems, similarly as in the case of underwater navigation, are not appropriate at larger distances (due to multipath, [8]) or in the cases when obstacles are present between the diver and the base station.

Preliminary research at the University of Zagreb Laboratory for Underwater Systems and Technologies (LABUST) has demonstrated that cooperation between autonomous marine vehicles and divers is the most appropriate solution to the above identified issues. We propose a concept illustrated in Fig. 1 that includes an autonomous surface platform with the ability to follow the diver thus significantly increasing their safety during underwater activities. The platform has the primary task to dynamically position itself above the diver, with the following results:

- There is no need for conventional marking of the diver area by using static buoys which will increase allowed diver operation area since the autonomous surface platform is always above the diver.
- A vertical acoustic communication channel is formed that ensures communication reliability. A reliable transmission of GPS coordinates to the diver is accomplished thus providing the diver with absolute GPS coordinates on the diver tablet.
- The diving supervisor has reliable data of the diver position and reliable communication between the diver and the diving supervisor is established through the vertical communication channel thus significantly increasing reactivity in the case of danger.

This paper focuses on the description of guidance and control algorithms for the autonomous surface platform which enable diver tracking. Section II describes basic technical characteristics of the platform and the overall concept while Section III presents mathematical models used for modeling the platform behaviour as well as diver tracking. Section IV describes the developed control and guidance algorithms with special attention devoted to the problem of diver tracking.

This work is supported by the Business Innovation Agency of the Republic of Croatia (BICRO) through the Proof of Concept programme.

The authors are with the University of Zagreb, Faculty of Electrical Engineering and Computing, LABUST - Laboratory for Underwater Systems and Technologies, Unska 3, Zagreb, Croatia nikola.miskovic at fer.hr

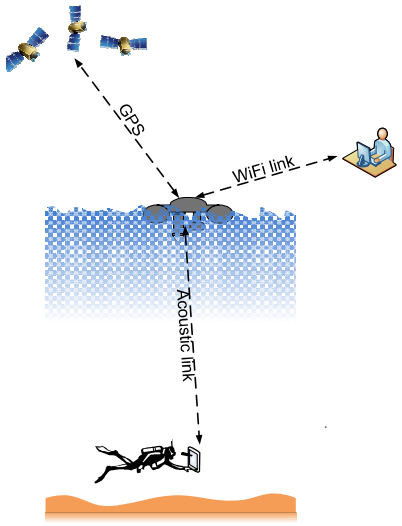

Fig. 1. Concept for diver navigation and monitoring consisting of an autonomous surface platform and a diver tablet.

Section V presents realistic simulation results. The paper is concluded in Section VI.

II. Technical Description

The proposed concept as a solution to the above mentioned issues consists of an autonomous surface platform and an underwater interface (tablet) carried by the diver, as shown in Fig. 1. The autonomous surface platform, that carries the international flag marking underwater activity, is overactuated with 4 thrusters forming the "X" configuration. This configuration enables motion in the horizontal plane under any orientation. The platform has been developed at LABUST and the current version is 0.35m high, 0.707m wide and long, as it is shown in Fig. 2, and it weighs approximately 25kg. The control computer (isolated from environmental disturbances inside the platform hull) is in charge of performing control and guidance tasks (dynamic positioning, path following, diver following) and all the data processing. Apart from the compass, batteries and CPUs, the platform is equipped with:

- a GPS for determining the platform position, and indirectly the diver position in the horizontal plane;
- Ultra Short Baseline (USBL) used to determine the position of the diver relative to the platform. The USBL is used simultaneously for localization and two-way data transmission via an acoustic link (the second modem is mounted on the diver);
- a wireless modem used to transmit data from the platform to the surface station, thus making the platform a router from the diver to the surface station where the diving supervisor is stationed.

III. Mathematical Modeling

A. The autonomous surface platform model

1) Dynamic model: Following the notation given in [5], dynamic model of the platform in the horizontal plane can

(a) (b)

Fig. 2. (a) CAD design and (b) the prototype of the autonomous surface platform developed in LABUST.

be described using the velocity vector $\boldsymbol{\nu} = \begin{bmatrix} u & v & r \end{bmatrix}^{\mathrm{T}}$ where u, v and r are surge, sway and yaw speed, respectively; and the vector of actuating forces and moments acting on the platform $\boldsymbol{\tau} = \begin{bmatrix} X & Y & N \end{bmatrix}^{\mathrm{T}}$ where X, Y are surge and sway forces and N is yaw moment. Both vectors are defined in the body-fixed (mobile) coordinate frame. The uncoupled dynamic model in the horizontal plane is given with (1) where $\mathbf{M}$ is a diagonal matrix with mass and added mass terms and $\mathbf{D}(\boldsymbol{\nu})$ is a diagonal matrix consisting of nonlinear hydrodynamic damping terms.

$$\mathbf{M}\dot{\boldsymbol{\nu}} = -\mathbf{D}(\boldsymbol{\nu}) + \boldsymbol{\tau} \tag{1}$$

Since the platform is designed to be symmetrical with respect to the x and y axes in the body fixed frame, the following forms of the two matrices are adopted: $\mathbf{M} = diag(\alpha_u, \alpha_u, \alpha_r)$, $\mathbf{D}(\boldsymbol{\nu}) = diag(\beta_u(u), \beta_u(v), \beta_r(r))$.

2) Kinematic model: The kinematic translatory equations for the platform motion in the horizontal plane on the sea surface is given with (2), where x and y are the position and ψ is the orientation of the platform in the Earth–fixed coordinate frame and $\mathbf{R}(\psi)$ is the rotation matrix.

$$\begin{bmatrix} \dot{x} \\ \dot{y} \end{bmatrix} = \underbrace{\begin{bmatrix} \cos\psi & -\sin\psi \\ \sin\psi & \cos\psi \end{bmatrix}}_{\mathbf{R}(\psi)} \begin{bmatrix} u \\ v \end{bmatrix} \tag{2}$$

Additional equation in the kinematic model is $\dot{\psi} = r$. The platform is overactuated, i.e. it can move in any direction in the horizontal plane by modifying the surge and sway speed, while attaining arbitrary orientation.

3) Actuator allocation: The actuator allocation matrix $\boldsymbol{\Phi}$ gives relation between the forces exerted by thrusters $\boldsymbol{\tau}_{\mathbf{i}} = \begin{bmatrix} \tau_1 & \tau_2 & \tau_3 & \tau_4 \end{bmatrix}^{\mathrm{T}}$ and the forces and moments $\boldsymbol{\tau}$ acting on the rigid body. Actuator configuration of the autonomous surface platform for diver tracking is given in Fig. 3 where $\delta = 45°$. The allocation matrix is given with (3).

$$\boldsymbol{\tau} = \underbrace{\begin{bmatrix} \cos 45° & \cos 45° & -\cos 45° & -\cos 45° \\ \sin 45° & -\sin 45° & \sin 45° & -\sin 45° \\ D & -D & -D & D \end{bmatrix}}_{\boldsymbol{\Phi}} \boldsymbol{\Phi}_{\mathbf{i}} \tag{3}$$

Since four actuators are used to control three degrees of freedom, this presents an overactuated system. This allows for the design of fault tolerant control algorithms,

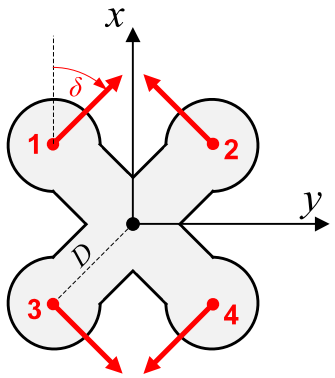

Fig. 3. Actuator configuration on the platform.

[7]. The inverse actuator allocation matrix cannot be found (since the matrix is not square), but a pseudoinverse $\mathbf{\Phi}^{\dagger} = \left(\mathbf{\Phi}^{\mathrm{T}}\mathbf{\Phi}\right)^{-1}\mathbf{\Phi}^{\mathrm{T}}$ can be calculated instead, [10].

Under the assumption that the feasible operating area of thrusters is $\boldsymbol{\tau}_{\mathbf{i}} \in (-\boldsymbol{\tau}_{\mathbf{i,min}}, \boldsymbol{\tau}_{\mathbf{i,max}})$, the feasibility space of the τ vector can be determined by using the allocation matrix (3) and it can be found in [7]. Under the assumption that the yaw moment N is zero, the feasible area takes a rhomboid form shown in Fig. 5. From here it is clear that both maximal surge and sway thrusts cannot be expected but a compromise is required. For the given thruster configuration, the maximal $\boldsymbol{\tau}$ values are given with and the minimum values are the same as the maximum (with a negative sign).

$$X_{\max} = Y_{\max} = \frac{N_{\max}}{D} = \sqrt{2}\left(\tau_{i,\max} + \tau_{i,\min}\right) \tag{4}$$

The main reason for choosing this configuration was to assure symmetry in the attainable thrust in the positive and negative direction. It should be mentioned that larger positive thrust could be achieved by inverting thrusters 3 and 4, at the expense of unsymmetrical feasibility area. More details about repercussions of this type of feasibility area on control windup are given in Section IV-B.

B. The diver model

Determining a simple dynamic model of a diver is practically impossible. For the specific case of the platform following a diver from the surface, a kinematic model of the diver projection on the surface horizontal plane will be sufficient. For that reason, the following states are defined: x_D and y_D are the positions and ψ_D is the orientation of the diver in the Earth-fixed coordinate frame, while u_D, v_D and r_D are the diver's linear and rotational velocities in the body-fixed frame, respectively. The kinematic model of the diver assumes that the diver cannot swim in the sway direction, i.e. $v_D = 0$ which leads to the following kinematic model:

$$\begin{bmatrix} \dot{x}_D \\ \dot{y}_D \\ \dot{\psi}_D \end{bmatrix} = \begin{bmatrix} \mathbf{R_D}\left(\psi_D\right) & 0 \\ 0 & 1 \end{bmatrix} \begin{bmatrix} u_D \\ r_D \end{bmatrix} \tag{5}$$

where $\mathbf{R_D}\left(\psi_D\right)$ is the diver's rotation matrix in the form

$$\mathbf{R_D}\left(\psi_D\right) = \begin{bmatrix} \cos\psi_D \\ \sin\psi_D \end{bmatrix}. \tag{6}$$

In order to enhance the estimation of the diver position, the assumption is made that the diver's surge speed u_D is constant and the yaw speed r_D has some dynamics determined with a time constant T_d. This results in the simplified dynamic model given with (7).

$$\begin{aligned} \dot{u}_D &= 0 \\ \dot{r}_D &= -T_D r_D \end{aligned} \tag{7}$$

C. The tracking model

The main requirement in the tracking task is to ensure that the distance between the platform and the diver in the horizontal plane defined with

$$\mathbf{d} = \begin{bmatrix} x - x_D \\ y - y_D \end{bmatrix} \tag{8}$$

converges to zero. The kinematic tracking model is then obtained by differentiating equation (8) resulting in

$$\dot{\mathbf{d}} = \mathbf{R}\left(\psi\right)\begin{bmatrix} u \\ v \end{bmatrix} - \mathbf{R_D}\left(\psi_D\right)u_D. \tag{9}$$

IV. Control and Guidance Design

A. Speed controller design

For the low–level, speed controller we choose a PI controller in the form

$$\boldsymbol{\tau} = \mathbf{K_P}\left(\boldsymbol{\nu}^* - \boldsymbol{\nu}\right) + \mathbf{K_I}\int\left(\boldsymbol{\nu}^* - \boldsymbol{\nu}\right)dt + \boldsymbol{\tau}_{\mathbf{F}} \tag{10}$$

where $\boldsymbol{\nu}^* = \begin{bmatrix} u^* & v^* & r^* \end{bmatrix}^{\mathrm{T}}$ are the desired linear and angular speeds of the platform, $\mathbf{K_P} = diag\left(K_{Pu}, K_{Pv}, K_{Pr}\right)$ and $\mathbf{K_I} = diag\left(K_{Iu}, K_{Iv}, K_{Ir}\right)$ are diagonal matrices with proportional and integral gains for individual degrees of freedom, respectively. The $\boldsymbol{\tau}_{\mathbf{F}}$ term represents additional action introduced in the controller to improve the closed loop behaviour. This action can be in the form $\boldsymbol{\tau}_{\mathbf{F}} = \mathbf{D}\left(\boldsymbol{\nu}\right)\boldsymbol{\nu}$ which results in the feedback linearization procedure where measured or estimated speeds are used to compensate for the nonlinearity in the process. The vehicle's speeds are often estimated since they are either difficult to measure or are unreliable. Faulty estimation can lead to instability of the closed loop due to the nature of feedback linearization. This is why it is much more convenient to use the reference speed signal instead of the measurements, i.e. $\boldsymbol{\tau}_{\mathbf{F}} = \mathbf{D}\left(\boldsymbol{\nu}^*\right)\boldsymbol{\nu}^*$ which leads to the feedforward action. It should be mentioned that, theoretically, both the feedback linearization and the feedforward approach result in the same closed loop behaviour. Controller parameters $\mathbf{K_P}$ and $\mathbf{K_I}$ can be calculated based on the desired closed loop characteristic equation as it is shown in [4]. These parameters will naturally depend on the parameters of the dynamic model which have to be identified. The dynamic model parameters of the platform that is addressed in this paper have been identified using the identification method based on self–oscillations reported in [6].

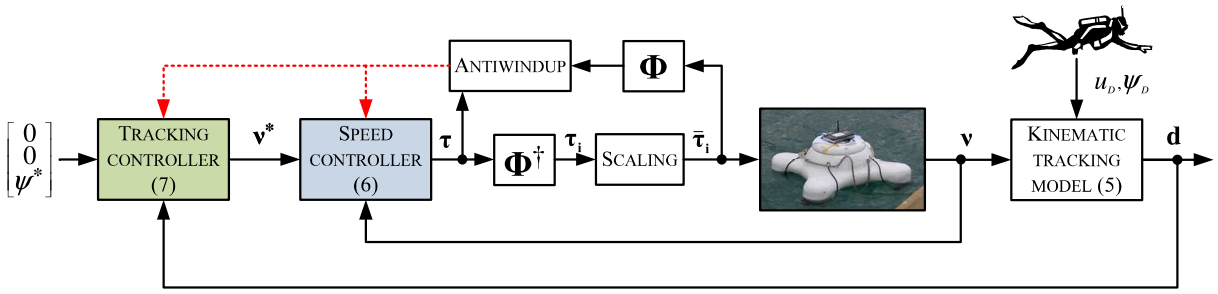

Fig. 4. Tracking and speed control scheme.

B. Guidance controller design

Since the platform is overactuated, the platform can move in a horizontal plane while keeping an arbitrary heading. For this reason, the high–level guidance controller is divided into the heading controller and the tracking controller design.

1) Heading controller: For the heading controller a PI structure is chosen since it compensates all environmental disturbances in the yaw degree of freedom. In addition to that, the integral action will compensate all the unmodelled dynamics and ensure convergence of the heading to the desired value ψ^*. The controller can be written in the form

$$r^* = -K_{P\psi}\left(\psi^* - \psi\right) - K_{I\psi}\int\left(\psi^* - \psi\right)dt \qquad (11)$$

where $K_{P\psi}$ and $K_{I\psi}$ are controller parameters chosen so that desired heading closed loop dynamics is achieved.

2) Tracking controller: With the tracking model given with (9), the PI control action in the form

$$\begin{bmatrix} u^* \\ v^* \end{bmatrix} = \mathbf{R}^{\mathrm{T}}(\psi)\left(-\mathbf{K_{P,d}}\mathbf{d} - \mathbf{K_{I,d}}\int \mathbf{d}dt\right) + \boldsymbol{\nu}_\mathbf{F}$$

where $\mathbf{K_{P,d}} = diag\begin{pmatrix} K_{P,dx}, & K_{P,dy} \end{pmatrix}$ and $\mathbf{K_{I,d}} = diag\begin{pmatrix} K_{I,dx}, & K_{I,dy} \end{pmatrix}$ are proportional and integral gain matrices, respectively, will ensure convergence of the distance $\mathbf{d}$ to the desired value $\mathbf{d}^* = \begin{bmatrix} 0 & 0 \end{bmatrix}^{\mathrm{T}}$. The $\boldsymbol{\nu}_\mathbf{F}$ is the feedforward action that can improve the behaviour of the tracking closed loop. If there is no feedforward action, i.e. $\boldsymbol{\nu}_\mathbf{F} = \begin{bmatrix} 0 & 0 \end{bmatrix}^{\mathrm{T}}$, and under the assumption that $\boldsymbol{\nu}^* \approx \boldsymbol{\nu}$, the relation between the desired distance and the influence of the diver motion is given with

$$\mathbf{d} = -\begin{bmatrix} \frac{s}{s^2+K_{p,dx}s+K_{I,dx}} & 0 \\ 0 & \frac{s}{s^2+K_{p,dy}s+K_{I,dy}} \end{bmatrix}\mathbf{R_D}(\psi_D)\,\nu_D.$$

Obviously, the PI controller without the feedforward action will guarantee convergence if the diver surge speed and heading are constant. However, tracking may be improved if feedforward action in the form $\boldsymbol{\nu}_\mathbf{F} = \mathbf{R}^{\mathrm{T}}(\psi)\,\mathbf{R_D}(\psi_D)\,\nu_D$ is introduced. The full tracking controller is given with (12).

$$\boldsymbol{\nu}^* = \begin{bmatrix} \mathbf{R}^{\mathrm{T}}(\psi)\left(-\mathbf{K_{P,d}}\mathbf{d} - \mathbf{K_{I,d}}\int \mathbf{d}\mathbf{d}\mathbf{t} + \mathbf{R_D}(\psi_\mathbf{D})\,\nu_\mathbf{D}\right) \\ -K_{P\psi}\left(\psi^* - \psi\right) - K_{I\psi}\int\left(\psi^* - \psi\right)dt \end{bmatrix} \qquad (12)$$

The proposed feedforward action requires the estimation of the diver surge speed and heading since they cannot be directly measured. It should also be mentioned that the desired dynamics of the low level control loop has to be chosen so that it is slower then the high level guidance loop.

3) Antiwindup: Antiwindup strategies for controllers with single outputs are available in literature, e.g. [3]. These single outputs have their physical limitations which are straightforward. However, in the case of an overactuated platform where the low level controller generates three outputs, the situation tends to get more complicating. The controller output $\boldsymbol{\tau}$ is distributed among individual thrusters that are constrained by their output thrust limitations. The controller output is constrained to a space determined by the limits of individual thrusters, i.e. $\tau_{i,max}$ and the configuration of thrusters given with allocation matrix Φ.

An illustrative example is given in Fig. 5 where controller output is assumed to take a form $\boldsymbol{\tau} = \begin{bmatrix} X & Y & 0 \end{bmatrix}^{\mathrm{T}}$ If the speed controller output pair (X, Y) is outside the feasible area, as it is shown with the red arrow in Fig. 5, the controller has exceeded the limit and integral windup will occur unless the antiwindup algorithms is implemented. By calculating the individual thrusts using $\boldsymbol{\tau}_\mathbf{i} = \boldsymbol{\Phi}^\dagger\boldsymbol{\tau}$, at least one of the thrusters will be saturated, i.e. $|\tau_i| > |\tau_{\max}|$.

There are two approaches that can be taken: the thrust limitation and the thrust scaling. The thrust limitation approach, given with Algorithm IV.1 saturates individual thrusts within their operating areas resulting in $\boldsymbol{\tau}_{\mathbf{i,lim}}$. If any of the thrusters is saturated, integration channels in all three controllers (surge, sway and yaw) are set to zero. The $\boldsymbol{\tau}_{\mathbf{i,lim}}$ is then multiplied with the allocation matrix resulting in $\boldsymbol{\tau}_{\mathbf{lim}} = \boldsymbol{\Phi}\boldsymbol{\tau}_{\mathbf{i,lim}}$. The resulting vector will be within the feasibility area but it will not be colinear with the original vector $\boldsymbol{\tau}$, as it is shown in Fig. 5 with the blue arrow. As a result, during the saturation, the platform will deviate from the desired path.

In order to avoid this effect, the thrust scaling approach given with Algorithm IV.2 is applied. Similar to the previous approach, if any of the thrusters is saturated, integration channels in all three controllers (surge, sway and yaw) are set to zero and the calculated vector $\bar{\boldsymbol{\tau}}_\mathbf{i}$ is scaled using (13) where $|\cdot|$ marks element–wise absolute value operator.

$$\bar{\boldsymbol{\tau}}_\mathbf{i} = \boldsymbol{\tau}_\mathbf{i}\frac{\tau_{\max}}{\max\left(|\boldsymbol{\tau}_\mathbf{i}|, \tau_{\max}\right)} \qquad (13)$$

The vector $\bar{\tau} = \boldsymbol{\Phi}\bar{\tau}_\mathbf{i}$ is then within the feasibility area and colinear with the original controller output $\boldsymbol{\tau}$, as it is shown in Fig. 5 with the green arrow.

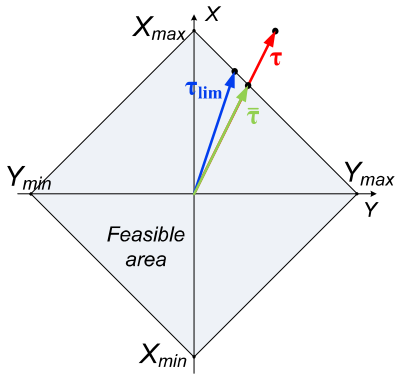

Fig. 5. Feasibility area of thrust vector τ with $N = 0$.

Algorithm IV.1: THRUSTER LIMITATION( )

$\boldsymbol{\tau_i} = \boldsymbol{\Phi}^{\dagger}\boldsymbol{\tau}$
$AW = 0$
for each τ_i
  do if $|\bar{\tau}_i| > |\tau_{max}|$
  then $\begin{cases} \tau_{i,lim} = \tau_{max} \\ AW += 1 \end{cases}$
  else $\tau_{i,lim} = \tau_i$
if $AW > 0$
  then all integrators $\leftarrow 0$

Algorithm IV.2: THRUSTER SCALING( )

$\boldsymbol{\tau_i} = \boldsymbol{\Phi}^{\dagger}\boldsymbol{\tau}$
$F = \frac{\tau_{\max}}{\max(|\boldsymbol{\tau_i}|, \tau_{\max})}$
$\bar{\boldsymbol{\tau}}_i = F \cdot \boldsymbol{\tau_i}$
$\bar{\boldsymbol{\tau}} = \boldsymbol{\Phi}\bar{\boldsymbol{\tau}}_i$
if $F > 1$
  then all integrators $\leftarrow 0$

The described antiwindup algorithm is to be used on the speed controller (10). In order to avoid windup in the guidance controller, its integration channel is set to 0 at the same time as the low level controller antiwindup is initiated. This principle of operation is schematically shown in Fig. 4.

V. SIMULATION RESULTS

The presented simulation results are obtained in the ROS environment, [1] and the UWSim underwater simulator, [2]. The simulations in this paper are used to demonstrate basic guidance and control behaviour in the ideal conditions, and the diver tracking algorithm with realistic simulation of the USBL and diver state estimation using extended Kalman filtering. During simulations, the heading of the platform was kept at a constant value to demonstrate how omnidirectional guidance can be achieved regardless of the desired heading.

A. Guidance and control algorithms

In order to demonstrate the behaviour of the guidance and control scheme illustrated in Fig. 4, the platform was dynamically positioned from the initial point $(5, 2)$ to the desired position $(0, 0)$. The results are shown in Fig. 6. From Fig. 6(a) it is clear that the proposed scaling of the speed controller outputs results in the shortest path while pure limitation of the thruster outputs causes unacceptable path deviation. Fig. 6(b) shows the performance of the implemented antiwindup Algorithm IV.2. Instantaneous reactivity to the controller output change is achieved and the speed controller outputs are always scaled so that the orientation of the requested thrust $\boldsymbol{\tau}^*$ is maintained.

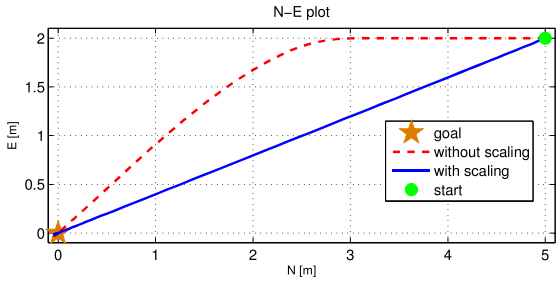

(a)

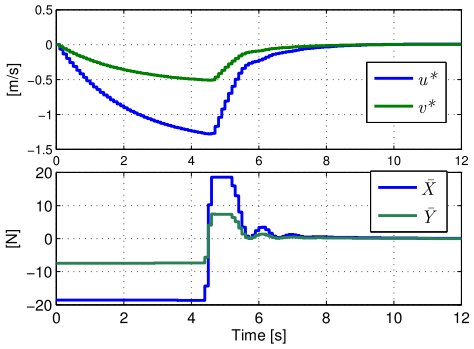

(b)

Fig. 6. (a) Comparison between paths with and without scaling, and (b) commanded speeds from the guidance controller and scaled commanded thrusts from the speed controller.

B. Diver tracking

The diver tracking simulation example is shown in Fig. 7(a) where the diver was attempting to follow a square path at an almost constant speed of 0.5m/s, with the exception around the corners where the speed decreases. True diver path during the experiment is shown in black dotted line. For the diver tracking simulation the USBL sensor was modeled with the error within 1m of the actual value. The diver position measurements, shown with red circles in Fig. 7(a), are available at a frequency of 1Hz while control is performed at 10Hz frequency. In order to minimize effects of measurement noise and low update frequency, an extended Kalman filter (EKF) was implemented. The filter was designed according to the models described in Section III. The EKF produced estimates of the diver's position, surge speed and yaw. The estimated diver path based on USBL measurements, is shown in Fig. 7(a) with green solid line. The estimated path is much smoother in comparison to the USBL measurements. However, due to the difference between the assumed diver model, and the real one, the estimated path is not completely smooth. The largest deviations are present near the corners

where the diver heading changes significantly. The path of the surface platform is shown in blue.

Fig. 7(b) shows the commanded thrust (blue solid line) during the diver tracking maneouvre. A comparison is given with the "ideal" thrust which is obtained by using real diver position, speed and orientation, and without using the EKF. The commanded thrust is naturally noisy due to the difference between the assumed diver model and the real one. Higher quality USBL measurements would lead to a smoother thruster command.

Fig. 7 shows the tracking error for the simulation example in blue colour. Most of the time, the error is below 1m, except in the cases when the diver is at the corners. Given the quality of measurements, we conclude that the tracking is satisfactory under the realistic simulation conditions.

VI. CONCLUSIONS AND DISCUSSION

It should be mentioned that the results described in the first part of this section are obtained with tracking and speed controllers tuned according to the desired closed loop characteristic equations. The tracking control loop has to be slower then the speed control loop in order to avoid instability. If the tracking control loop is set to be faster, then the tracking error can be reduced, as it is shown in Fig. 7 in green line. However, this improvement comes at an expense of higher thrust activity. Simulations have shown that the slower tracking loop gives an average tracking error of 0.887m, while the faster loop decreases this error to 0.696m. However, the faster loop will consume about 16% more energy of the thrusters in comparison to the slower loop tracking, and the thrusters will exhibit more jittering.

The work presented in this paper has demonstrated that the concept of using an autonomous surface platform for diver tracking is feasible. Based on USBL measurements, diver position, speed and orientation can be estimated with sufficient precision. Further work will be focused on performing experiments at sea with real divers. Special attention will be devoted to tuning of tracking controllers in order to obtain an optimal ration between the tracking error and energy consumption.

REFERENCES

[1] http://www.ros.org.

[2] http://www.irs.uji.es/uwsim/.

[3] K.J. Åström and T. Hägglund. *PID controllers*. Setting the standard for automation. International Society for Measurement and Control, 1995.

[4] M. Caccia, M. Bibuli, R. Bono, and G. Bruzzone. Basic navigation, guidance and control of an unmanned surface vehicle. *Autonomous Robots*, 2008.

[5] T.I. Fossen. *Guidance and Control of Ocean Vehicles*. John Wiley & Sons, New York, NY, USA, 1994.

[6] N. Miskovic, Z. Vukic, M. Bibuli, G. Bruzzone, and M. Caccia. Fast in-field identification of unmanned marine vehicles. *Journal of Field Robotics*, 28(1):101–120, 2011. doi: 10.1002/rob.20374.

[7] Edin Omerdic and Geoff Roberts. Thruster fault diagnosis and accommodation for open-frame underwater vehicles. *Control Engineering Practice*, 12(12):1575 – 1598, 2004. <ce:title>Guidance and control of underwater vehicles</ce:title>.

[8] M. Stojanovic and J. Preisig. Underwater acoustic communication channels: Propagation models and statistical characterization. *Communications Magazine, IEEE*, 47(1):84 –89, january 2009.

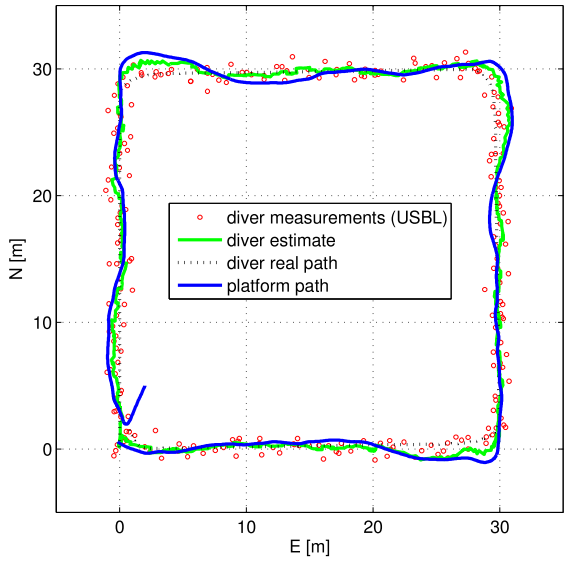

(a)

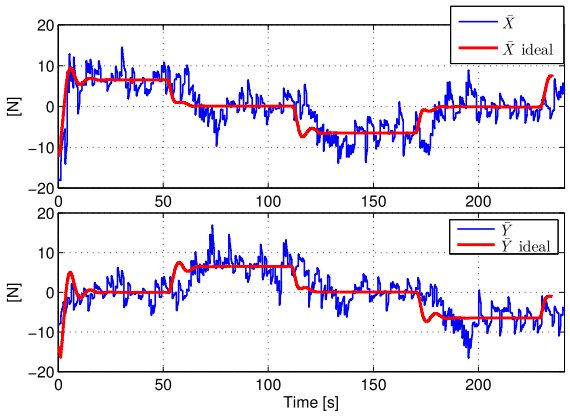

(b)

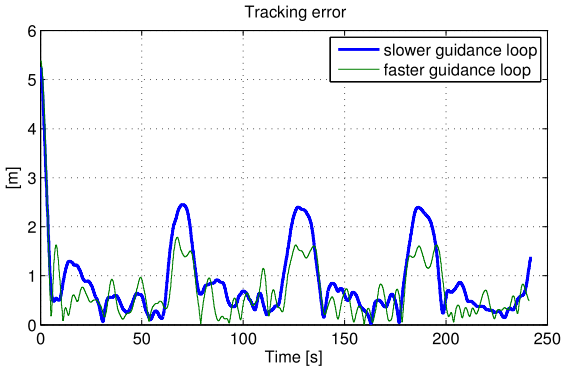

(c)

Fig. 7. Simulation of the diver performing following the square pattern while being tracked by the surface platform. (a) shows the paths, 7(b) shows the commanded thrusts compared to the ideal case, and shows tracking errors for two cases of tracking controllers.